Syntheses, Characterisation and Crystal Structures of Metal Complexes of a Novel 1,2-Dithiolate Ligand, 6,7-Dihydro-6-methylene-5*H*-1,4-dithiepine-2,3-dithiol†

Adam Charlton,[a] Allan E. Underhill,[a] Akiko Kobayashi[b] and Hayao Kobayashi[c]

[a] *Department of Chemistry, University of Wales, Bangor, Gwynedd LL57 2UW, UK*

[b] *Department of Chemistry, Faculty of Science, University of Tokyo, Hongo, Bunkyo-ku, Tokyo 113, Japan*

[c] *Department of Chemistry, Faculty of Science, Toho University, Funabashi, Chiba 274, Japan*

A series of $[NR_4][M(dpdt)_2]$ (R = Bu, M = Ni **2**, Au **3** or Cu **4**; R = Me, M = Ni **5**; H_2dpdt = 6,7-dihydro-6-methylene-5*H*-1,4-dithiepine-2,3-dithiol) complexes have been synthesized. Magnetic susceptibility measurements indicate that the gold **3** and copper **4** complexes are diamagnetic, whilst the nickel salt **2** is paramagnetic over the temperature range studied (290–22 K). The solution redox properties are consistent with a 1,2-dithiolene structure for these compounds. Single crystal X-ray analysis on compounds **2**–**4** revealed crystal-packing structures consisting of two crystallographically independent $[M(dpdt)_2]^-$ moieties possessing square-planar geometry, in which there are no intermolecular S···S contacts shorter than the sum of the van der Waals radii (3.70 Å).

The emergence of molecular electronics as an important area within materials science in recent years has led to an intense period of investigation into materials exhibiting novel electrical properties.[1] Transition-metal complexes of sulfur donor ligands, particularly those of the anionic $[M(dmit)_2]$ (H_2dmit = 4,5-dimercapto-1,3-dithiole-2-thione) series of compounds have been the focus of considerable research interest, due to the high electrical conductivities[2] and superconducting behaviour[3] observed in some of the derivatives.

The major problem associated with many of these quasi one-dimensional systems is their inherent instability at low temperatures, due to the Peierls distortion which results in a metal-to-insulator transition, and an insulating ground state rather than superconductivity. Recent work suggests that suppression of this distortion down to low temperatures can be achieved by increasing the two- and three-dimensional interactions within the crystal lattice. Increasing the amount of peripheral sulfur associated with the ligand framework is one way of achieving this, because intermolecular contacts are strengthened due to the presence of the additional S···S intermolecular interactions within the sulfur framework.[4] This is particularly apparent in compounds such as [ttf][{Ni(dmit)$_2$}$_2$][5] (ttf = tetrathiafulvalene) and the first ambient pressure superconducting $[M(dmit)_2]$ derivative [α-ettf][Ni(dmit)$_2$] [ettf = (ethylenedithio)tetrathiafulvalene].[6]

There are essentially three structural modifications that can be made to improve upon the high electrical conductivities observed in the anionic $[M(dmit)_2]$ complexes: (1) change the central metal, (2) change the associated counter cation or (3) change the ligand framework. The first two modifications have been studied extensively, but the latter has received less attention.[7]

We now report the synthesis, physical properties and molecular structure of a range of metal complexes of a new multisulfur ligand system, 6,7-dihydro-6-methylene-5*H*-1,4-dithiepine-2,3-dithiol (H_2dpdt)].

Results and Discussion

Synthesis of the Ligand Precursor and the Monoanionic Metal Complexes **2**–**5**.—The synthetic route employed in the preparation of the $[NR_4][M(dpdt)_2]$ complexes is outlined in Scheme 1 (R = Bu, M = Ni **2**, Au **3** or Cu **4**; R = Me, M = Ni **5**).

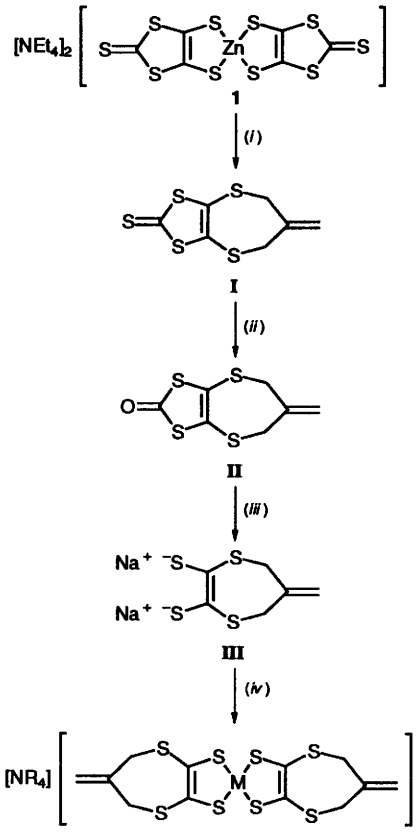

Scheme 1 R = Bu, M = Ni **2**, Au **3** or Cu **4**; R = Me, M = Ni **5**. Reagents and conditions: (*i*) $H_2C{=}C(CH_2Cl)_2$, dry thf, 20 °C, 16 h; (*ii*) $Hg(O_2CMe)_2$, CH_2Cl_2–$MeCO_2H$, 20 °C, 16 h; (*iii*) NaOEt–EtOH, 20 °C, 1 h; (*iv*) NR_4Br then $MCl_x{\cdot}Y\,H_2O$

† *Supplementary data available:* see Instructions for Authors, *J. Chem. Soc., Dalton Trans.*, 1995, Issue 1, pp. xxv–xxx.

Table 1 Analytical and physical data for complexes **2–5**

Complex	M.p./°C	Colour	*m/z*[a]	Analysis (%)[b] C	H	N
2	152–153	Brown	470 (45)	46.85 (47.15)	6.50 (6.70)	1.75 (1.95)
3	126–128	Golden brown	609 (100)	39.50 (39.50)	5.55 (5.65)	1.50 (1.65)
4	114–115	Red	475 (45)	46.60 (46.80)	6.70 (6.70)	1.95 (1.95)
5	250 (decomp.)	Brown	*c*	35.55 (35.25)	4.55 (4.40)	2.35 (2.55)

[a] FAB, percentage abundance in parentheses. [b] Calculated values in parentheses. [c] Data not available.

Starting from the readily available $[NEt_4]_2[Zn(dmit)_2]$[8] **1**, reaction with 3-chloro-2-(chloromethyl)prop-1-ene gave the thioketone derivative **I** in 70–80% yield. Reaction of **I** with mercury(II) acetate yielded the ligand precursor **II** as a pale orange crystalline solid. Both compounds were characterised by elemental analysis, ^1H NMR, mass spectrometry and IR and UV/VIS spectroscopy (see Experimental section).

Reaction of **II** with sodium ethoxide under argon gave the air-sensitive disodium salt **III**, which was then allowed to react with the appropriate metal chloride and tetraalkylammonium bromide salt, to form the corresponding metal 1,2-dithiolene complexes.

In the case of the nickel and gold complexes **2** and **3**, addition of the metal chloride salt to the clear yellow solution of **III** and NBu_4Br resulted in the formation of brown precipitates. Recrystallisation of the isolated solids yielded the pure complexes as crystalline compounds.

The preparation of $[NBu_4][Cu(dpdt)_2]$ **4** involved the dropwise addition of $CuCl_2{\cdot}2H_2O$ in ethanol to a solution of **III** in ethanol. The red solution was stirred for 1 h before the addition of the NBu_4Br solution. The isolated product was recrystallised to give the complex as a red crystalline solid.

Single crystals of all three complexes **2–4**, suitable for X-ray diffraction studies, were obtained by slow evaporation of concentrated acetone–hexane mixtures. The salt $[NMe_4][Ni(dpdt)_2]$ **5** was also prepared, but it was not possible to isolate single crystals of this compound. Analytical and mass spectral data for complexes **2–5** are presented in Table 1.

X-Ray Structural Studies.—*(a) Molecular structure of the* $[M(dpdt)_2]^-$ *monoanions.* In order to gain insight into the structure/property relationships in these materials, the crystal structures of compounds **2–4** were determined. Figs. 1 and 2 show the molecular structure of the $[Cu(dpdt)_2]^-$ and $[Ni(dpdt)_2]^-$ monoanions, and as can be seen they are similar. Bond lengths and angles are given in Tables 2 and 3 respectively.

The molecular structure of $[Cu(dpdt)_2]^-$ is composed of a planar CuC_4S_4 core, with the terminal C_4H_6 groups distorted from planarity giving rise to a chair-type conformation. Within the copper–sulfur core, the average Cu–S distance is 2.174 Å which is similar to the reported value of 2.170 Å in $[NBu_4][Cu(mnt)_2]$[9] (H_2mnt = dicyanoethylene-1,2-dithiol), and the average value of 2.181 Å reported by Vance *et al.*[10] for $[NMe_4][Cu(dddt)_2]$ (H_2dddt = 5,6-dihydro-1,4-dithiine-2,3-dithiol). The S–Cu–S angle in $[Cu(dpdt)_2]^-$ is 91.99° which is close to the ideal angle of 90° for a square coplanar geometry.

The atoms C(3), C(4), C(5) and C(6) deviate from the plane of the CuS_4 core by 1.65–2.12 Å, and the terminal C(4)–C(6) bond distance is 1.324(8) Å. There are no short S···S intermolecular contacts less than the sum of the van der Waals radii (3.70 Å).

The planar nature of the central CuC_4S_4 fragment in $[Cu(dpdt)_2]^-$ is in contrast to the crystal structures of other

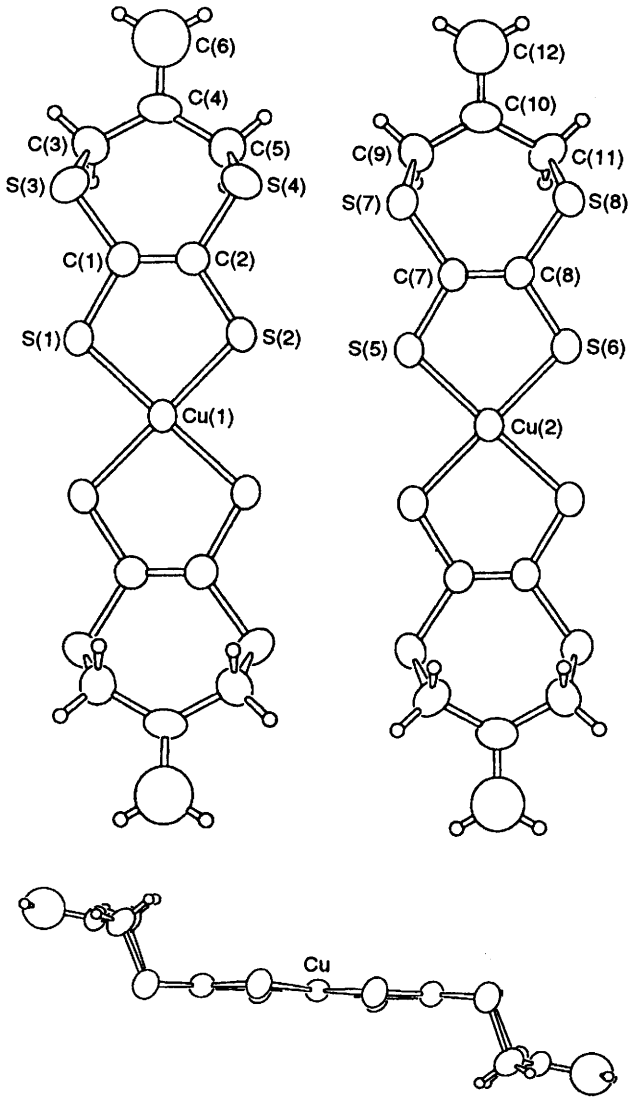

Fig. 1 Molecular structure of $[Cu(dpdt)_2]^-$ and labelling of the non-hydrogen atoms

copper 1,2-dithiolenes such as $[NBu_4][Cu(dddt)_2]$[10] and the dianionic complex $[epy]_2[Cu(dmit)_2]$[11] (epy = *N*-ethylpyridinium). In these materials, the geometry around the copper atom is distorted from planarity around the metal centre due to crystal-packing forces, with dihedral angles between the planes of 29 and 57.3° respectively. The bulky chair-type conformation of the $[Cu(dpdt)_2]^-$ units presumably limits the effect of these crystal-packing forces, enabling the CuC_4S_4 core to remain planar.

The molecular structure of $[Ni(dpdt)_2]^-$ is essentially the same as for the copper complex, with the anion unit being planar except for the terminal C_4H_6 moieties which deviate from planarity, giving rise to a chair-type conformation. This type of conformation has been reported for a structurally related complex, $[NBu_4][Ni(C_4H_4S_5)_2]$ prepared by Kato *et al.*[12] and more recently for the neutral $[Ni(dpdt)_2]$ complex.[13]

The square coplanar NiC_4S_4 core in compound **2** displays D_{2h} symmetry in common with other nickel 1,2-dithiolenes, within which the average Ni–S and C–C (chelate ring) bond distances are 2.138(7) and 1.360(8) Å respectively.

Table 4 lists selected average bond lengths and angles for several nickel 1,2-dithiolene complexes for comparison. It can be seen that the distances and angles are essentially the same for all four compounds, with the central S–Ni–S angle being close to the ideal value of 90° for square coplanar geometry.

Table 2 Intramolecular bond lengths (Å) and angles (°) with estimated standard deviations (e.s.d.s) in parentheses for $[NBu_4][Cu(dpdt)_2]$ **4**

Cu(1)–S(1)	2.180(2)	S(7)–C(7)	1.744(5)
Cu(1)–S(2)	2.168(2)	S(7)–C(9)	1.821(6)
Cu(2)–S(5)	2.179(2)	S(8)–C(8)	1.745(5)
Cu(2)–S(6)	2.175(2)	S(8)–C(11)	1.819(7)
S(1)–C(1)	1.743(6)	C(1)–C(2)	1.341(7)
S(2)–C(2)	1.741(6)	C(3)–C(4)	1.485(8)
S(3)–C(1)	1.747(5)	C(4)–C(5)	1.472(8)
S(3)–C(3)	1.810(6)	C(4)–C(6)	1.324(8)
S(4)–C(2)	1.746(5)	C(7)–C(8)	1.344(6)
S(4)–C(5)	1.825(6)	C(9)–C(10)	1.480(8)
S(5)–C(7)	1.733(5)	C(10)–C(11)	1.480(8)
S(6)–C(8)	1.746(5)	C(10)–C(12)	1.313(8)
S(1)–Cu(1)–S(2)	92.21(7)	S(3)–C(3)–C(4)	116.1(4)
S(5)–Cu(2)–S(6)	91.77(7)	C(3)–C(4)–C(5)	118.2(5)
Cu(1)–S(1)–C(1)	102.8(2)	C(3)–C(4)–C(6)	121.4(6)
Cu(1)–S(2)–C(2)	102.8(2)	C(5)–C(4)–C(6)	120.3(6)
C(1)–S(3)–C(3)	102.0(3)	S(4)–C(5)–C(4)	114.3(4)
C(2)–S(4)–C(5)	101.1(3)	S(5)–C(7)–S(7)	115.5(3)
C(2)–S(4)–C(5)	101.1(3)	S(5)–C(7)–C(8)	120.9(4)
Cu(2)–S(5)–C(7)	103.1(2)	S(7)–C(7)–C(8)	123.6(4)
Cu(2)–S(6)–C(8)	102.8(2)	S(6)–C(8)–S(8)	114.3(3)
C(7)–S(7)–C(9)	103.4(3)	S(6)–C(8)–C(7)	120.7(4)
C(8)–S(8)–C(11)	101.7(3)	S(8)–C(8)–C(7)	125.0(4)
S(1)–C(1)–S(3)	115.4(3)	S(7)–C(9)–C(10)	114.8(4)
S(1)–C(1)–C(2)	120.5(4)	C(9)–C(10)–C(11)	118.5(5)
S(3)–C(1)–C(2)	124.1(4)	C(9)–C(10)–C(12)	121.4(6)
S(2)–C(2)–S(4)	114.7(3)	C(11)–C(10)–C(12)	120.1(6)
S(2)–C(2)–C(1)	121.4(4)	S(8)–C(11)–C(10)	114.8(4)
S(4)–C(2)–C(1)	123.7(4)		

Table 3 Intramolecular bond lengths (Å) and angles (°) with e.s.d.s in parentheses involving the non-hydrogen atoms in $[NBu_4][Ni(dpdt)_2]$ **2**

Ni(1)–S(1)	2.143(2)	S(7)–C(11)	1.811(8)
Ni(1)–S(2)	2.130(2)	S(7)–C(10)	2.792(9)
Ni(2)–S(5)	2.144(2)	S(8)–C(7)	1.754(7)
Ni(2)–S(6)	2.137(2)	S(8)–C(8)	2.757(7)
S(1)–C(1)	1.726(7)	S(8)–C(9)	1.806(8)
S(1)–C(2)	2.670(7)	S(8)–C(10)	2.777(9)
S(2)–C(1)	2.677(7)	N(1)–C(13)	1.53(1)
S(2)–C(2)	1.729(7)	C(1)–C(2)	1.356(8)
S(3)–C(1)	1.754(7)	C(1)–C(3)	2.77(1)
S(3)–C(2)	2.751(8)	C(2)–C(5)	2.75(1)
S(3)–C(3)	1.801(8)	C(3)–C(4)	1.49(1)
S(4)–C(1)	2.743(8)	C(3)–C(5)	2.55(1)
S(4)–C(2)	1.746(7)	C(3)–C(6)	2.45(1)
S(4)–C(4)	2.782(8)	C(4)–C(5)	1.49(1)
S(4)–C(5)	1.801(8)	C(4)–C(6)	1.31(1)
S(5)–C(7)	2.666(7)	C(5)–C(6)	2.42(1)
S(5)–C(8)	1.720(7)	C(7)–C(8)	1.364(8)
S(6)–C(7)	1.720(7)	C(7)–C(9)	2.78(1)
S(6)–C(8)	2.678(7)	C(8)–C(11)	2.80(1)
S(7)–C(7)	2.757(7)	C(9)–C(12)	2.42(1)
S(7)–C(8)	1.750(7)		
S(1)–Ni(1)–S(2)	91.89(8)	C(3)–C(4)–C(5)	117.9(7)
S(5)–Ni(2)–S(6)	91.46(8)	C(3)–C(4)–C(6)	122.2(8)
Ni(1)–S(1)–C(1)	104.2(3)	C(5)–C(4)–C(6)	119.8(8)
Ni(1)–S(2)–C(2)	104.3(3)	S(4)–C(5)–C(4)	115.2(5)
C(1)–S(3)–C(3)	102.4(3)	S(6)–C(7)–S(8)	116.1(4)
C(2)–S(4)–C(5)	101.8(3)	S(6)–C(7)–C(8)	120.1(6)
Ni(2)–S(5)–C(8)	104.6(2)	S(8)–C(7)–C(8)	123.8(6)
Ni(2)–S(6)–C(7)	104.4(2)	S(5)–C(8)–S(7)	116.6(4)
C(8)–S(7)–C(11)	103.5(3)	S(5)–C(8)–C(7)	119.2(5)
S(1)–C(1)–S(3)	116.5(4)	S(5)–C(8)–C(11)	127.8(4)
S(1)–C(1)–C(2)	119.6(6)	S(7)–C(8)–C(7)	124.1(6)
S(3)–C(1)–C(2)	123.9(6)	S(8)–C(9)–C(10)	115.2(5)
S(2)–C(2)–S(4)	116.2(4)	S(7)–C(11)–C(10)	115.0(5)
S(2)–C(2)–C(1)	119.9(6)	C(9)–C(10)–C(12)	120.8(9)
S(4)–C(2)–C(1)	123.8(6)	C(12)–C(10)–C(11)	121.0(8)
S(3)–C(3)–C(4)	116.7(5)		

Table 4 Selected average bond lengths (Å) and angles (°) for several nickel 1,2-dithiolene complexes

Compound	Ni–S	C–C (chelate ring)	S–Ni–S	Ref.
$[NBu_4][Ni(ddt)_2]$[a]	2.142	1.350	91.5	12
$[NBu_4][Ni(dddt)_2]$	2.146(6)	1.34(2)	90.0(2)	14(*a*), 14(*b*)[b]
$[NBu_4][Ni(dmit)_2]$	2.156(3)	1.39[a]	93.2(1)	15
$[NBu_4][Ni(dpdt)_2]$	2.138(7)	1.360(8)	88.3(3)	This work

[a] H_2ddt = 1,4-Dithiine-2,3-dithiol; standard deviations not reported. [b] For details of the crystal structure of $[NBu_4][Ni(dddt)_2]$ for which no details of bond lengths or angles were published see ref. 14(*b*).

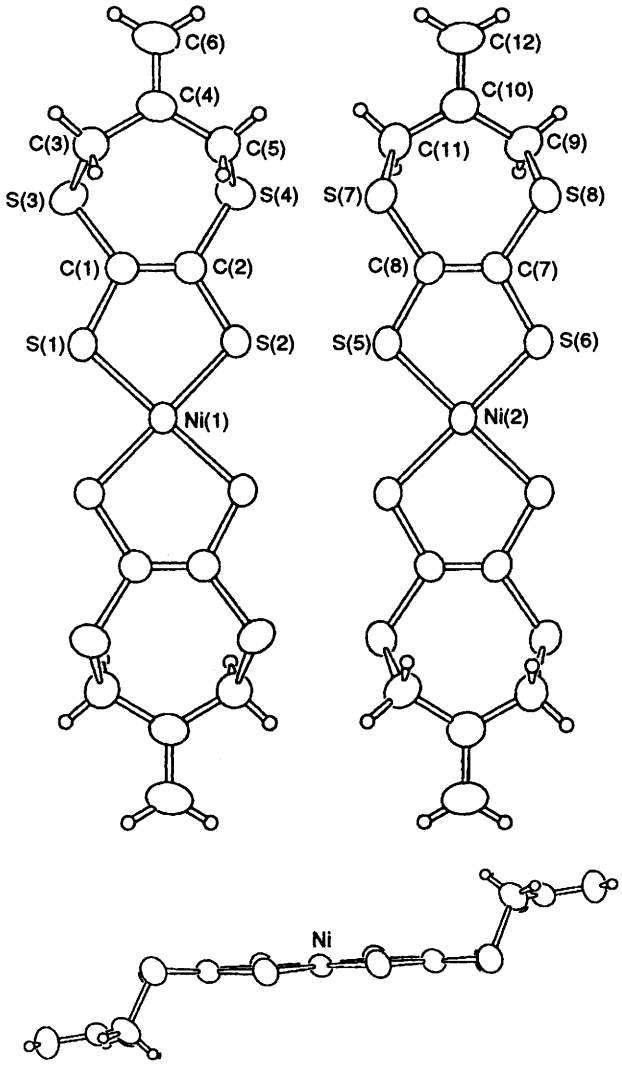

Fig. 2 Molecular structure of $[Ni(dpdt)_2]^-$ and labelling of the non-hydrogen atoms

Comparisons can also be made between the relevant bond lengths in the monoanionic and neutral $[Ni(dpdt)_2]$ complexes. Oxidation of the $[NBu_4][Ni(dpdt)_2]$ salt to the neutral $[Ni(dpdt)_2]$ compound leads to a decrease in the Ni–S bond length from 2.138(7) to 2.122(6) Å, but an increase in the chelate ring C–C bond distance from 1.360(8) to 1.399(6) Å.[13] This is due to the increased dithioketone nature of the chelating ligand in the neutral complex compared to the monoanionic nickel compound, in which the ligand can be considered as an ethylenedithiolate species. Consequently, in the neutral

complex, the chelate ring C–C bond distance is longer because it is a perturbed C=C bond. This type of observation has been reported previously by Schrauzer,[16] with similar decreases in the Ni–S bond length being reported by Valade *et al.*[17] for the $[Ni(dmit)_2]^{x-}$ series.

The molecular structure of the $[Au(dpdt)_2]^-$ monoanion is different from that of both the nickel and copper complexes, due to the fact that the anion moieties adopt two different conformations in the unit cell. The molecular geometries of these $[Au(dpdt)_2]^-$ monoanions are shown in Fig. 3. Bond lengths and angles are given in Table 5.

One of the molecules adopts a chair-type conformation similar to that which is present in the unit cell of the nickel complex **2** [the *exo* conformation, see Fig. 3(*a*)]. The average Au–S distance in the square coplanar AuC_4S_4 core is 2.312(2) Å and the chelate ring C–C bond distance is 1.339(8) Å. The seven-membered C_5S_2 rings adopt chair-type conformations, with the terminal methylene groups in equatorial positions. The terminal C=C bond distance is 1.317(9) Å.

In the second *endo* conformation the AuC_4S_4 core is again planar with average Au–S and chelate ring C–C bond distances of 2.311(2) and 1.326(3) Å respectively. The main structural difference is that the terminal methylene groups are in axial rather than equatorial positions relative to the C_5S_2 rings [see Fig. 3(*b*)]. The terminal C=C bond distance is 1.29(1) Å.

The energy difference between the two different conformations of $[Au(dpdt)_2]^-$ in the unit cell was calculated using a Burchart universal forcefield in a Molecular Simulations Cerius 3.1 package. The *exo* conformation was found to be 86.5 kJ mol^{-1} higher in energy than the *endo*.

The mean Au–S and chelate ring C–C distances in $[NBu_4][Au(dpdt)_2]$ **3** compare well with the respective values of 2.322 and 1.314 Å reported for the crystal structure of $[NBu_4][Au(dmit)_2]$.[18] The average S–Au–S angles in $[NBu_4][Au(dpdt)_2]$ and $[NBu_4][Au(dmit)_2]$ are 90.4 and 91.4° respectively.

(*b*) *Crystal structures of the* $[NBu_4][M(dpdt)_2]$ *salts.* The crystal structure of $[NBu_4][Cu(dpdt)_2]$ **4** reveals the presence of two crystallographically independent anion moieties within the unit cell. One group of molecules form a stack structure aligned along the *b* axis, whilst a second stack lies almost perpendicular to the first (see Fig. 4). The $[Cu(dpdt)_2]^-$ units are on the centre of symmetry. Within a stack, the shortest

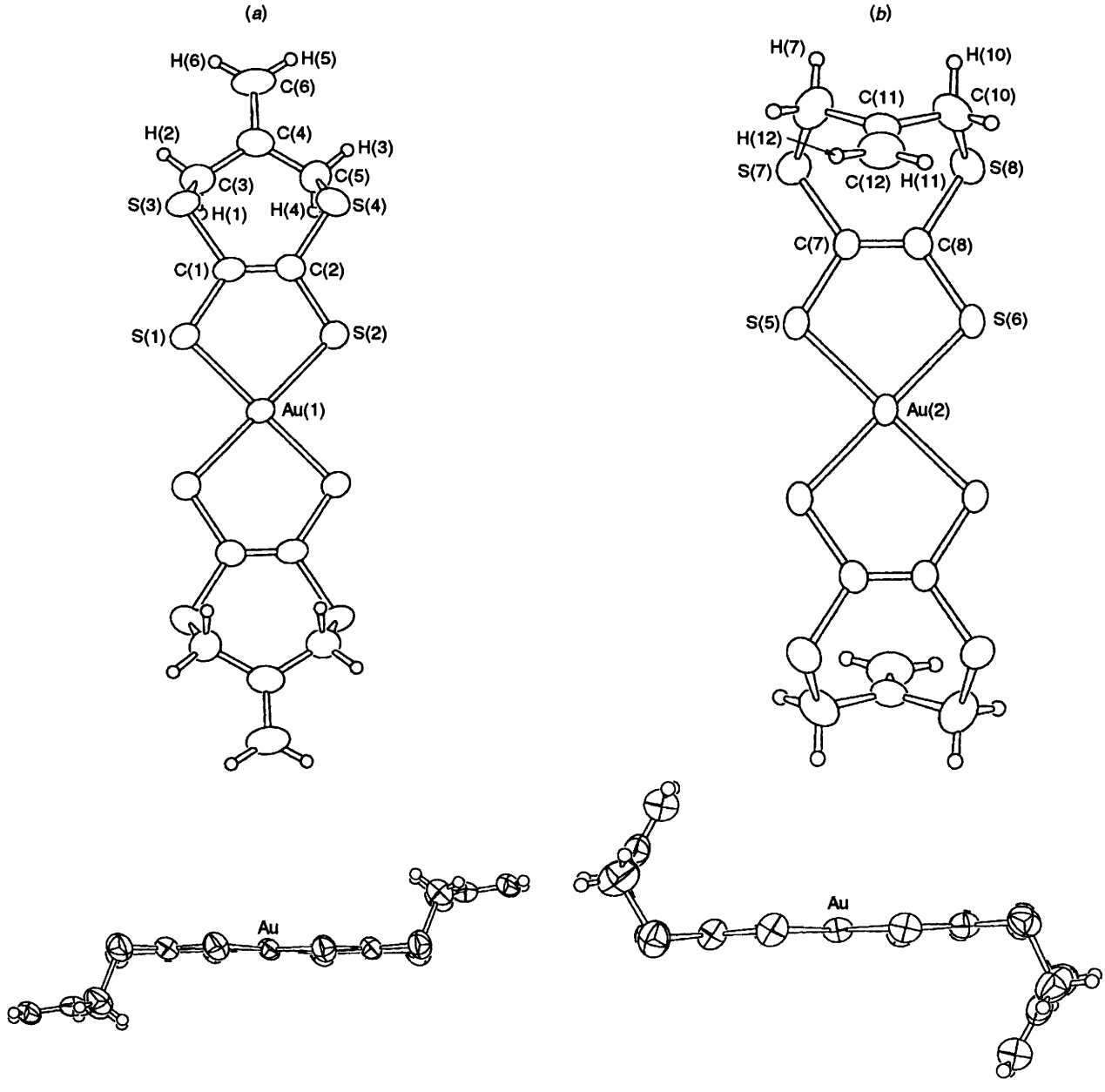

Fig. 3 Molecular structure of the *exo* (*a*) and *endo* (*b*) conformations of $[Au(dpdt)_2]^-$, showing the labelling of the atoms

Table 5 Intramolecular bond lengths (Å) and angles (°) with e.s.d.s in parentheses for $[NBu_4][Au(dpdt)_2]$ **3**

Au(1)–S(1)	2.311(2)	S(8)–C(10)	1.797(8)
Au(1)–S(2)	2.313(2)	C(1)–C(2)	1.339(8)
Au(2)–S(5)	2.312(2)	C(3)–C(4)	1.49(1)
Au(2)–S(6)	2.311(2)	C(3)–C(5)	2.53(1)
S(1)–C(1)	1.744(7)	C(3)–C(6)	2.45(1)
S(2)–C(2)	1.753(7)	C(4)–C(5)	1.48(1)
S(3)–C(1)	1.764(6)	C(4)–C(6)	1.317(9)
S(3)–C(3)	1.821(7)	C(5)–C(6)	2.44(1)
S(4)–C(2)	1.750(7)	C(7)–C(8)	1.326(7)
S(4)–C(5)	1.826(7)	C(9)–C(10)	2.54(1)
S(5)–C(7)	1.751(6)	C(9)–C(11)	1.49(1)
S(6)–C(8)	1.754(6)	C(9)–C(12)	2.43(1)
S(7)–C(7)	1.764(6)	C(10)–C(11)	1.48(1)
S(7)–C(9)	1.806(8)	C(10)–C(12)	2.42(1)
S(8)–C(8)	1.754(6)	C(11)–C(12)	1.29(1)
S(1)–Au(1)–S(2)	89.75(6)	C(3)–C(5)–C(6)	59.0(3)
S(5)–Au(2)–S(6)	89.36(6)	C(4)–C(5)–C(6)	27.3(4)
Au(1)–S(1)–C(1)	101.4(2)	C(3)–C(6)–C(4)	31.4(4)
Au(1)–S(2)–C(2)	102.0(2)	C(3)–C(6)–C(5)	62.4(3)
C(1)–S(3)–C(3)	101.1(3)	C(4)–C(6)–C(5)	31.0(4)
C(2)–S(4)–C(5)	102.5(3)	S(5)–C(7)–S(7)	114.3(3)
Au(2)–S(5)–C(7)	101.9(2)	S(5)–C(7)–C(8)	123.6(5)
Au(2)–S(6)–C(8)	102.1(2)	S(7)–C(7)–C(8)	122.2(5)
C(7)–S(7)–C(9)	103.5(3)	S(6)–C(8)–S(8)	114.1(3)
C(8)–S(8)–C(10)	101.7(3)	S(6)–C(8)–C(7)	123.0(5)
S(1)–C(1)–S(3)	113.0(4)	S(8)–C(8)–C(7)	122.9(5)
S(1)–C(1)–C(2)	124.5(5)	S(7)–C(9)–C(10)	101.5(4)
S(3)–C(1)–C(2)	122.6(5)	S(7)–C(9)–C(11)	115.4(5)
S(2)–C(2)–S(4)	113.6(4)	S(7)–C(9)–C(12)	123.1(5)
S(2)–C(2)–C(1)	122.3(5)	C(10)–C(9)–C(11)	31.3(4)
S(4)–C(2)–C(1)	124.1(5)	C(10)–C(9)–C(12)	58.4(3)
S(3)–C(3)–C(4)	115.0(5)	C(11)–C(9)–C(12)	27.1(4)
S(3)–C(3)–C(5)	102.5(4)	S(8)–C(10)–C(9)	100.2(4)
S(3)–C(3)–C(6)	120.7(4)	S(8)–C(10)–C(11)	116.8(5)
C(4)–C(3)–C(5)	31.3(4)	S(8)–C(10)–C(12)	126.7(4)
C(4)–C(3)–C(6)	27.4(4)	C(9)–C(10)–C(11)	31.5(4)
C(5)–C(3)–C(6)	58.6(3)	C(9)–C(10)–C(12)	58.5(3)
C(3)–C(4)–C(5)	117.1(6)	C(11)–C(10)–C(12)	27.0(4)
C(3)–C(4)–C(6)	121.2(8)	C(9)–C(11)–C(10)	117.1(7)
C(5)–C(4)–C(6)	121.6(7)	C(9)–C(11)–C(12)	121.2(8)
S(4)–C(5)–C(3)	100.8(3)	C(10)–C(11)–C(12)	121.6(8)
S(4)–C(5)–C(4)	114.8(5)	C(9)–C(12)–C(10)	63.1(4)
S(4)–C(5)–C(6)	121.7(4)	C(9)–C(12)–C(11)	31.7(5)
C(3)–C(5)–C(4)	31.6(4)	C(10)–C(12)–C(11)	31.4(5)

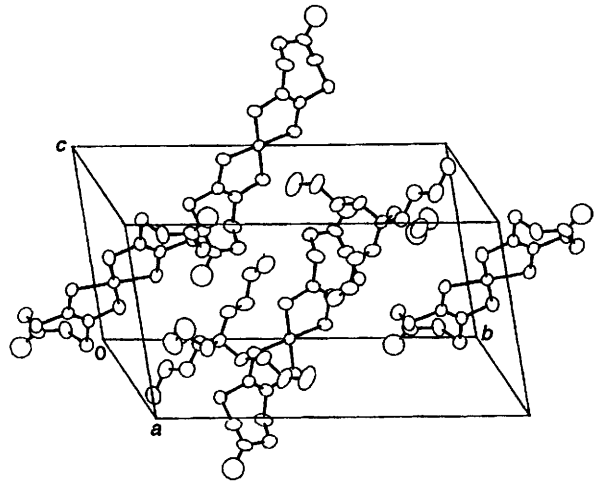

Fig. 4 Crystal packing of $[NBu_4][Cu(dpdt)_2]$ **4** facing the *bc* plane

Cu · · · Cu and S · · · S intermolecular interactions were 10.263 and 9.255 Å respectively. However, the closest interstack, intermolecular S · · · S contact was considerably shorter at 7.420 Å, with the shortest Cu · · · Cu distance being 10.60 Å.

The presence of stacks of $[Cu(dpdt)_2]^-$ anions along the *b* axis is similar to the reported structure of the unit cell of $[NMe_3H][Cu(dddt)_2]$.[10] It was however noted that this complex possessed shorter intermolecular S · · · S contacts (4.47 Å) than the complex containing the smaller $[NMe_3H]^+$ cation as the counter ion. It is apparent that the incorporation of smaller counter ions in the crystal lattice does not guarantee closer intermolecular interactions. The value of 10.263 Å quoted for the intrastack, intermolecular Cu · · · Cu distance in $[NBu_4][Cu(dpdt)_2]$ compares well with the value of 10.1 Å quoted for the same interatomic distance in $[NMe_3H][Cu(dddt)_2]$.

The crystal structure of $[NBu_4][Ni(dpdt)_2]$ **2** is similar to that of the copper complex, with the unit cell containing two crystallographically independent types of molecule (see Figs. 5 and 6). One group of molecules forms a stack structure along the *a* axis, whilst a second stack lies almost perpendicular to the first. The shortest Ni · · · Ni and S · · · S intermolecular distances are 10.29 and 3.991 Å respectively, the latter being considerably greater than the sum of the van der Waals radii (3.70 Å).

The structure is similar to that reported for one polymorph of $[NBu_4][Ni(dddt)_2]$.[14] This latter compound crystallises in two polymorphs, one in a triclinic cell and one in a monoclinic cell. The triclinic cell contains anions arranged in segregated stacks aligned approximately along the *a* axis and anions orientated roughly perpendicular to the stacks. The latter anions are well-separated from each other in contrast to those in the stacks.

The crystal structure of $[NBu_4][Au(dpdt)_2]$ **3**, in common with both the nickel and copper complexes, consists of two independent stacks of molecules, one located along the *c* axis, and the other one almost perpendicular to the first (see Fig. 7). Within the stack of the *endo* conformers, the shortest Au · · · Au and S · · · S intermolecular contacts are 10.144 and 6.447 Å. The closest interstack distances of *exo* conformers are S · · · S at 4.482 Å and Au · · · Au at 11.058 Å. This structure is in contrast to that of $[NBu_4][Au(dmit)_2]$,[18] which contains a one-dimensional chain of anions along the *c* axis with weak S · · · S contacts, leading to semiconducting behaviour.

Magnetic Susceptibility Studies.—Magnetic susceptibility measurements indicate that $[NBu_4][Ni(dpdt)_2]$ **2** is paramagnetic over the temperature range 294–22 K, this being consistent with the presence of isolated monomer units in the crystal lattice. The gold and copper complexes **3** and **4**, were, however, diamagnetic over the same temperature range.

The difference in the magnetic properties between complex **2** and **3** and **4** can be understood in terms of the relative occupancies of the frontier orbitals (highest and next highest occupied molecular orbitals, HOMO and NHOMO) in these materials (see Fig. 8). In compound **2**, the electronic configuration of the nickel atom results in the presence of an unpaired electron in the HOMO [see Fig. 8(*b*)], leading to paramagnetic behaviour. There is no spin coupling between these paramagnetic units because, as indicated by the crystal structure of **2**, there is minimal interaction between adjacent $[Ni(dpdt)_2]^-$ anions due to the presence of the bulky NBu_4^+ cations.

The HOMOs of both the copper and gold complexes **3** and **4** are, however, doubly occupied [see Fig. 8(*d*)], resulting in diamagnetic behaviour.

Near-infrared Properties.—Complex $[NBu_4][Ni(dpdt)_2]$ **2** when dissolved in dichloromethane exhibited an intense near-infrared band at 930 nm (see Fig. 9). This band is characteristic of neutral and monoanionic nickel 1,2-dithiolenes, and is assigned to an NHOMO–HOMO, π–π^* transition.[19] This intense band is absent in the corresponding copper and gold complexes **3** and **4**, because in these compounds the HOMO is completely filled [see Fig. 8(*d*)]. This low-energy transition is also absent in the isoelectronic (considering valence electrons

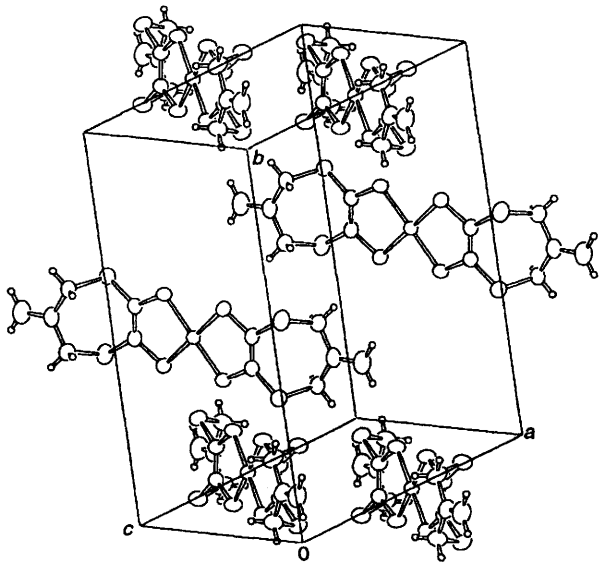

Fig. 5 Crystal packing of $[NBu_4][Ni(dpdt)_2]$ **2** facing the *ab* plane. The NBu_4^+ cations have been omitted for clarity

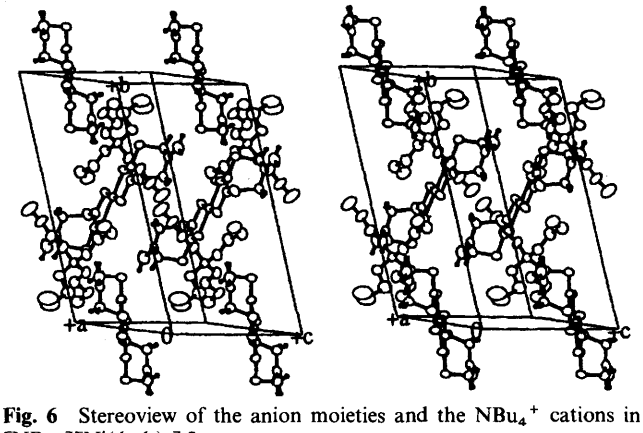

Fig. 6 Stereoview of the anion moieties and the NBu_4^+ cations in $[NBu_4][Ni(dpdt)_2]$ **2**

only) dianionic nickel 1,2-dithiolene complexes[16] [see Fig. 8(*c*)]. The UV/VIS spectroscopic data for compounds **2**–**5** are presented in Table 6.

Redox Properties.—The electrochemical properties of complexes **2**–**5** were studied using cyclic voltammetry (Table 7).[20] The cyclic voltammogram of complex **2** showed two reversible redox waves corresponding to the $[M(dithiolene)_2]^{2-} \rightleftharpoons [M(dithiolene)_2]^{-1}$ (E_1) and $[M(dithiolene)_2]^{1-} \rightleftharpoons [M(dithiolene)_2]^0$ (E_2) couples (see Fig. 10); E_1 and E_2 represent peak oxidation potentials. This is consistent with the classical shape of the cyclic voltammograms of nickel 1,2-dithiolenes such as $[NBu_4][Ni(dmit)_2]$.[21] When the scan rate was reduced from 200 to 100 mV s^{-1} and the scan cycled repeatedly, both redox couples remained reversible.

The voltammogram of complex **3** showed three irreversible peaks, the first two corresponding to oxidation from the dianion through to the neutral species, as for **2**, whilst the third peak (E_3) may be assigned to the formation of a cationic $[Au(dpdt)_2]^{6+}$ species, similar to the $[Au(dddt)_2]^{6+}$ (H_2dddt = 5,6-dihydro-1,4-dithiine-2,3-dithiol) complexes reported by Yagubskii *et al.*[22] (see Fig. 11). Schultz *et al.*[14] also observed a third peak in the cyclic voltammogram of the $[Au(dddt)_2]$ complex, which was assigned to the $[Au(dddt)_2]^0 \rightleftharpoons [Au(dddt)_2]^+$ redox couple, although this was described as quasi-reversible. The irreversibility of the three peaks in the voltammogram of $[NBu_4][Au(dpdt)_2]$ is probably attributable to precipitation of

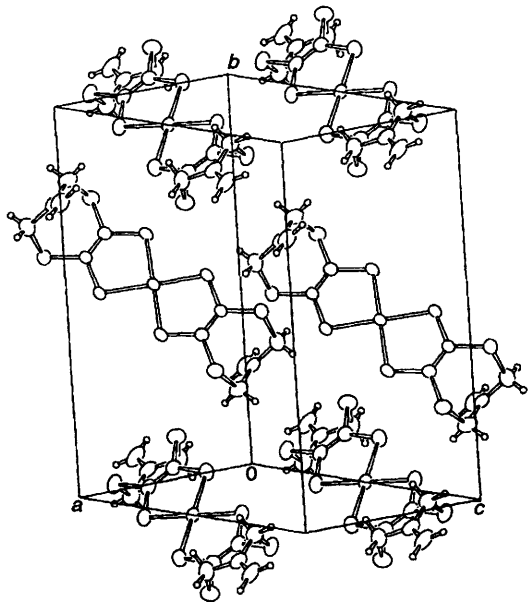

Fig. 7 Crystal packing of $[NBu_4][Au(dpdt)_2]$ **3** facing the *ab* plane. The NBu_4^+ cations have been omitted for clarity

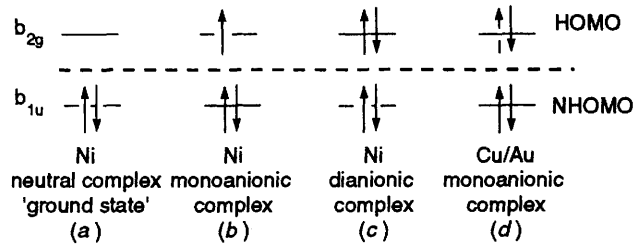

Fig. 8 Relative occupancies of the frontier orbitals in the $[M(dpdt)_2]^{x-}$ complexes

the oxidised species modifying the surface of the working electrode. The irreversible oxidation of a series of substituted $[Au(bdt)_2]^-$ (H_2bdt = benzene-1,2-dithiol) complexes (see Fig. 11), in a variety of solvents was also recently reported by Schiødt *et al.*[23] during an investigation into the redox chemistry of these materials.

The voltammogram of complex **4** shows one reversible wave at −0.63 V corresponding to the dianion to monoanion couple. At more positive potentials (+0.47 V) a second irreversible wave was observed, corresponding to the monoanion–neutral couple. As with complex **3**, it is apparent that the oxidised species plates out on the working electrode, causing irreversibility of the wave. This is in close agreement with previous results on the redox properties of the $[NBu_4][Cu(dddt)_2]$ monoanionic complex.[10]

General Discussion.—A comparison of the half-wave ($E_{\frac{1}{2}}$) potentials for the nickel complexes illustrated in Fig. 11 is presented in Table 8 ($E_{\frac{1}{2}}$ values are defined as the midpoint between the redox peak potentials).

It can be seen from Table 8 that the order of stability of the dianionic species is: $dmit^{2-} > ddt^{2-} > dpdt^{2-} > dddt^{2-}$. Therefore the dianionic $[M(dmit)_2]^{2-}$ complexes should be the most stable, while those of the dddt and dpdt ligands should be more readily oxidised to the corresponding monoanions. This is consistent with the experimental evidence, since the $[M(dmit)_2]^{2-}$ dianions are stable in air, and require treatment with iodine, or prolonged exposure to air in solution before they are converted to the monoanions.[25] In contrast, the $[M(dddt)_2]^{x-}$ salts were generally isolated as the monoanions, although if oxygen was excluded from the reaction the dianionic species could be prepared, although they were readily oxidised

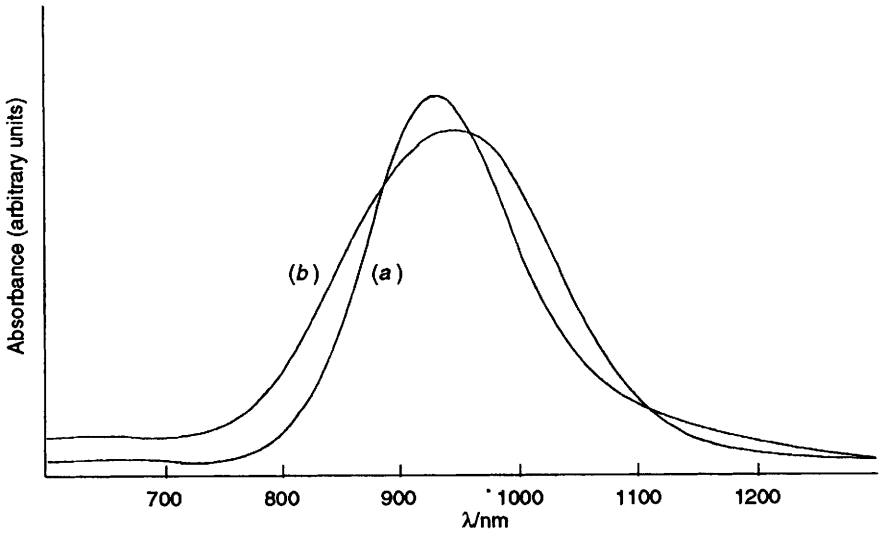

Fig. 9 The near-infrared spectra of (*a*) $[NBu_4][Ni(dpdt)_2]$ **2** (1.2×10^{-4} mol dm^{-3}) and (*b*) $[Ni(dpdt)_2]$ **6** (4.2×10^{-5} mol dm^{-3}) recorded in dichloromethane

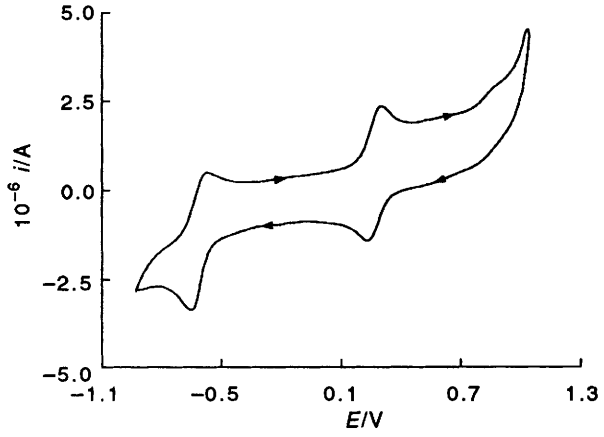

Fig. 10 Cyclic voltammogram of $[NBu_4][Ni(dpdt)_2]$ **2** recorded at 200 mV s^{-1}, in MeCN solution, with 0.1 mol dm^{-3} NBu_4PF_6 as supporting electrolyte

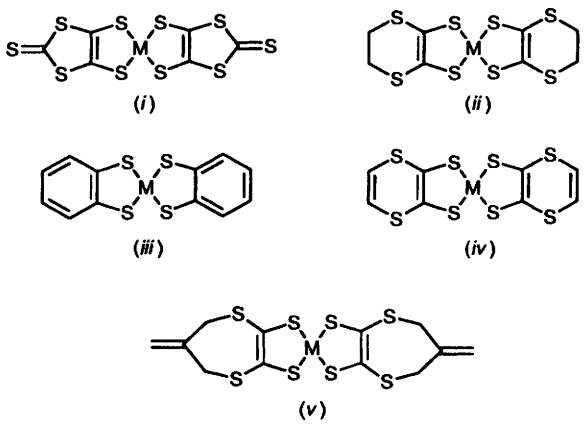

Fig. 11 Structures of the metal 1,2-dithiolenes: (*i*) $[M(dmit)_2]$, (*ii*) $[M(dddt)_2]$, (*iii*) $[M(bdt)_2]$, (*iv*) $[M(ddt)_2]$, (*v*) $[M(dpdt)_2]$

Table 6 Solution UV/VIS absorption data for complexes **2–5***

Complex	λ/nm (ε/dm^3 mol^{-1} cm^{-1})
2	930 (10 313), 395 (11 040), 319 (20 773), 233 (23 661)
3	339 (16 530), 247 (31 203)
4	438 (21 946), 281 (25 323), 232 (34 841)
5	930 (10 500), 400 (4 090), 272 (20 791)

* Recorded in dichloromethane.

Table 7 Cyclic voltammetric data for complexes **2–5**[a]

Complex	E_1/V	ΔE_p/mV	E_2/V	ΔE_p/mV	E_3/V
2	−0.58	70	+0.26	40	—
3	+0.63[b]	—	+1.28[b]	—	+1.54[b]
4	−0.63	90	+0.47[b]	—	—
5	−0.62	80	+0.27[b]	—	—

[a] Recorded in MeCN *vs.* SCE, 0.1 mol dm^{-3} NBu_4PF_6, 200 mV s^{-1}. [b] Irreversible.

back to the monoanionic species.[26] The $[M(dpdt)_2]^{x-}$ salts were all isolated as the monoanionic species.

The increased stability of the $[M(dmit)_2]^{2-}$ dianions is probably attributable to the electron withdrawing thioketone groups in the dmit ligand, which can readily accommodate the larger number of valence electrons. This type of reasoning is

Table 8 Values for $E_{\frac{1}{2}}$ for selected nickel 1,2-dithiolene complexes; redox process is $[Ni(dithiolene)_2]^{2-} \overset{E_1}{\rightleftharpoons} [Ni(dithiolene)_2]^{1-} \overset{E_2}{\rightleftharpoons} [Ni(dithiolene)_2]^{0}$ for all complexes

Compound	$E_{\frac{1}{2}}$/V		ΔE/V
$[Ni(ddt)_2]^{2-}$[a]	−0.51	+0.06	0.57
$[Ni(dddt)_2]^{2-}$[a]	−0.69	+0.06	0.75
$[Ni(dmit)_2]^{2-}$[a]	−0.13	+0.22	0.35
$[Ni(dpdt)_2]^{2-}$[b]	−0.62	+0.24	0.86

[a] See ref. 24. Recorded in MeCN *vs.* SCE. [b] Recorded in MeCN, 0.1 mol dm^{-3} NBu_4PF_6, 200 mV s^{-1}.

consistent with the trends reported by Olson *et al.*[20a] in their studies on the electrochemical properties of various substituted metal 1,2-dithiolene complexes. Removal of the terminal thioketone groups as in the dpdt ligand results in the overall reduction in the electron-withdrawing ability of the sulfur framework, and hence a lowering in the stability of the dianionic species.

The ΔE values in Table 8 can be considered an approximate guide to the relative intramolecular coulombic repulsion that emerges in these nickel 1,2-dithiolene systems, with the lowest values of ΔE reflecting the most effective delocalisation of charge on the molecule. The values imply that in terms of this

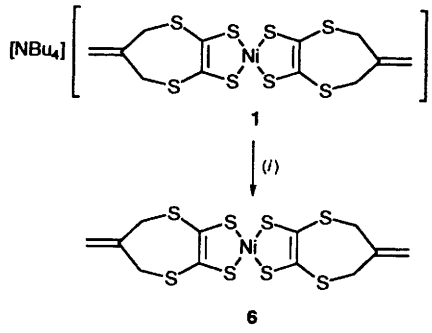

Scheme 2 (*i*) Iodine–Me_2CO, room temperature, 30 min

repulsion energy, the $[Ni(ddt)_2]^{x-}$ complex is intermediate between $[Ni(dmit)_2]^{x-}$, which shows the most effective charge delocalisation and $[Ni(dddt)_2]^{x-}$. This presumably reflects the weakly electron-withdrawing ability of the terminal alkene moiety in the ddt ligand.

The ΔE value for $[Ni(dpdt)_2]^{2-}$ is much higher than that observed for the other compounds, which suggest that this anion possesses large intramolecular coulombic repulsions, resulting from greater localisation of the electrons. In the solid state this is likely to reduce the extent of intermolecular π-orbital overlap through S···S contacts and this in turn might be expected to lower the electrical conductivity of any salts containing the $[M(dpdt)_2]^{x-}$ unit.

Oxidation of $[NBu_4][Ni(dpdt)_2]$ **2** to the neutral $[Ni(dpdt)_2]$ compound (see Scheme 2) was possible using either electrochemical[13] or chemical methods. The monoanionic complex was allowed to react with iodine dissolved in acetone, resulting in the precipitation of compound $[Ni(dpdt)_2]$ **6** as a green solid. The low solubility of **6** in common solvents prevented a detailed physical investigation of this compound, although the solution near-infrared spectrum recorded in dichloromethane exhibited an intense peak at 945 nm ($\ln \varepsilon$ = 10.46) [Fig. 9(*b*)]. High quality crystals of **6** were isolated and the crystal structure and electrical conductivity of this material have been reported elsewhere.[13]

Preliminary work regarding the preparation of partially oxidised $[Ni(dpdt)_2]^{x-}$ complexes, using electrocrystallisation techniques, has to date yielded semiconducting, rather than metallic compounds.[13]

Conclusion

A consideration of the electrochemical and structural data available for the $[NBu_4][M(dpdt)_2]$ compounds suggests that removal of the terminal thione moieties present in the $[M(dmit)_2]^-$ complexes, and the inclusion of CH_2 spacer units to yield the $[M(dpdt)_2]^-$ complexes, results in a molecular system in which intramolecular coulombic repulsions are increased. The close stacking of the metal complex anions observed in the $[M(dmit)_2]^{x-}$ series is no longer present in the $[M(dpdt)_2]^{x-}$ system.

It is thought that the non-planarity of the $[M(dpdt)_2]$ anions, whilst not precluding the formation of conducting stacked structures may affect the ability to delocalise electrons through the crystal lattice due to these increased intramolecular repulsions. Indeed, recent studies on extended tetrathiafulvalene (ttf) systems indicate that as long as the conjugated π-framework is planar, then planarity of the rest of the molecule is not a necessary pre-requisite for attainment of a conducting state.[27]

Further studies are underway to prepare electrically conducting $[M(dpdt)_2]^{x-}$ complexes, and to synthesize related systems in which intramolecular coulombic repulsions are reduced through the attachment of suitable groups onto the basic $[M(dpdt)_2]^-$ framework.

Table 9 Fractional atomic coordinates of $[NBu_4][Cu(dpdt)_2]$ **4** with e.s.d.s in parentheses

Atom	*x*	*y*	*z*
Cu(1)	0	$\frac{1}{2}$	0
Cu(2)	$\frac{1}{2}$	0	$\frac{1}{2}$
S(1)	0.112 0(2)	0.387 14(8)	−0.026 0(2)
S(2)	−0.108 8(2)	0.507 58(8)	−0.223 9(1)
S(3)	0.098 9(2)	0.277 55(8)	−0.263 7(2)
S(4)	−0.120 1(2)	0.407 0(1)	−0.472 2(2)
S(5)	0.491 7(2)	0.117 13(8)	0.532 7(2)
S(6)	0.673 6(2)	−0.021 76(8)	0.698 5(2)
S(7)	0.618 6(2)	0.214 86(8)	0.768 9(2)
S(8)	0.806 0(2)	0.067 66(9)	0.945 9(2)
N(1)	0.571 2(5)	0.249 6(3)	0.227 4(5)
C(1)	0.039 7(6)	0.367 3(3)	−0.205 6(6)
C(2)	−0.053 7(6)	0.419 4(3)	−0.289 9(5)
C(3)	0.207 9(6)	0.289 7(3)	−0.360 0(6)
C(4)	0.129 1(6)	0.317 2(4)	−0.502 4(6)
C(5)	0.043 2(7)	0.392 8(4)	−0.514 4(6)
C(6)	0.139 6(8)	0.276 3(4)	−0.615 9(7)
C(7)	0.609 7(6)	0.125 5(3)	0.701 9(5)
C(8)	0.687 6(6)	0.066 0(3)	0.774 0(5)
C(9)	0.801 6(7)	0.218 5(3)	0.793 5(7)
C(10)	0.911 0(6)	0.185 1(3)	0.921 3(7)
C(11)	0.945 1(6)	0.104 5(3)	0.927 1(7)
C(12)	0.978 3(7)	0.225 2(4)	1.027 3(7)
C(13)	0.565 4(8)	0.286 8(4)	0.368 1(7)
C(14)	0.448 5(8)	0.349 3(4)	0.365 9(8)
C(15)	0.438 1(9)	0.378 7(5)	0.509 9(9)
C(16)	0.551(1)	0.408 9(5)	0.607(1)
C(17)	0.453 6(7)	0.207 4(4)	0.164 9(8)
C(18)	0.449 2(7)	0.162 0(4)	0.031 6(8)
C(19)	0.337 9(7)	0.118 0(4)	−0.016(1)
C(20)	0.329 6(9)	0.074 2(4)	−0.148(1)
C(21)	0.551 8(7)	0.303 7(3)	0.124 3(6)
C(22)	0.654 5(7)	0.351 7(4)	0.167 8(7)
C(23)	0.622 0(8)	0.402 4(4)	0.053 8(8)
C(24)	0.724(1)	0.449 8(5)	0.092(1)
C(25)	0.717 3(7)	0.197 5(4)	0.253 8(7)
C(26)	0.748 2(9)	0.133 4(5)	0.331(1)
C(27)	0.908(1)	0.087 8(5)	0.356(1)
C(28)	0.992(1)	0.112 4(7)	0.462(1)

Experimental

Complex $[NEt_4]_2[Zn(dmit)_2]$ was prepared according to literature methods,[8] and recrystallised from acetone–methanol prior to use. The monoanionic $[M(dpdt)_2]^-$ complexes were prepared under argon due to the air sensitivity of compound **III**. Ethanol was dried by refluxing over magnesium turnings followed by distillation, and then stored over 4 Å molecular sieves under argon prior to use.

Proton NMR spectra were recorded on a Bruker AC250 spectrometer in $CDCl_3$, and referenced internally relative to $SiMe_4$ (δ 0). Elemental analyses were obtained using a Carlo Erba 1106 elemental analyser and trifluoroacetanilide as a reference standard, whilst mass spectra were recorded on Finnigan 1020 (GC-MS) and Kratos M550 RF machines in the negative-ion mode (EI), using 3-nitrobenzyl alcohol as the matrix. The UV/VIS and near-infrared spectra were recorded on Pye-Unicam PU8800 and Perkin-Elmer Lambda 9 spectrophotometers respectively.

Cyclic voltammetry measurements were recorded on an EG&G Princeton Applied Research model 264A polarographic analyser/stripping voltammeter connected to an EG&G Condecon 300 controller. All measurements were carried out in acetonitrile which had been predried over K_2CO_3 and redistilled from CaH_2, using NBu_4PF_6 (0.1 mol dm^{-3}) as the background electrolyte. All potentials are quoted in volts relative to a saturated calomel electrode (SCE) using a Pt button working electrode and Pt wire counter electrode. Typically, scan rates of 200 mV s^{-1} were used.

Table 10 Fractional atomic coordinates of $[NBu_4][Ni(dpdt)_2]$ **2** with e.s.d.s in parentheses

Atom	x	y	z
Ni(1)	0	$\frac{1}{2}$	$\frac{1}{2}$
Ni(2)	$\frac{1}{2}$	0	0
S(2)	0.0249(2)	0.3898(1)	0.3877(2)
S(2)	0.2196(2)	0.5068(1)	0.6065(2)
S(3)	0.2590(2)	0.2787(1)	0.3939(3)
S(4)	0.4699(2)	0.4078(1)	0.6152(2)
S(5)	0.5336(2)	−0.1154(1)	−0.0080(2)
S(6)	0.6976(2)	0.0208(1)	0.1664(2)
S(7)	0.7662(2)	−0.2152(1)	0.1214(2)
S(8)	0.9450(2)	−0.0676(1)	0.3073(2)
N(1)	0.2270(7)	0.7515(3)	0.0717(7)
C(1)	0.2021(7)	0.3688(4)	0.4535(8)
C(2)	0.2884(7)	0.4209(4)	0.5480(7)
C(3)	0.3574(9)	0.2908(4)	0.2877(8)
C(4)	0.5003(9)	0.3171(5)	0.3673(8)
C(5)	0.5140(8)	0.3931(5)	0.4552(9)
C(6)	0.612(1)	0.2765(5)	0.359(1)
C(7)	0.7727(7)	−0.0648(4)	0.1876(7)
C(8)	0.6993(7)	−0.1255(4)	0.1120(7)
C(9)	0.9282(8)	−0.1050(5)	0.4462(8)
C(12)	1.028(1)	−0.2256(5)	0.481(1)
C(10)	0.923(1)	−0.1854(5)	0.4139(8)
C(11)	0.7940(9)	−0.2192(4)	0.305(1)
C(13)	0.163(1)	0.7946(5)	−0.047(1)
C(14)	0.032(1)	0.8389(6)	−0.048(1)
C(15)	−0.018(1)	0.8827(5)	−0.163(1)
C(16)	−0.149(1)	0.9257(6)	−0.169(1)
C(17)	0.256(1)	0.8035(5)	0.219(1)
C(18)	0.333(1)	0.8667(7)	0.247(1)
C(19)	0.358(2)	0.9137(8)	0.414(2)
C(20)	0.462(2)	0.888(1)	0.490(2)
C(21)	0.367(1)	0.7126(6)	0.063(1)
C(22)	0.362(1)	0.6512(6)	−0.052(1)
C(23)	0.507(1)	0.6217(6)	−0.060(1)
C(24)	0.605(1)	0.5906(6)	0.052(1)
C(25)	0.1253(9)	0.6967(5)	0.056(1)
C(26)	0.168(1)	0.6488(5)	0.156(1)
C(27)	0.058(1)	0.5959(6)	0.125(1)
C(28)	0.096(2)	0.5487(8)	0.222(1)

Table 11 Fractional atomic coordinates of $[NBu_4][Au(dpdt)_2]$ **3** with e.s.d.s in parentheses

Atom	x	y	z
Au(1)	0	0	$\frac{1}{2}$
Au(2)	$\frac{1}{2}$	$\frac{1}{2}$	0
S(1)	0.161 7(2)	−0.000 1(1)	0.407 6(2)
S(2)	0.028 4(2)	0.122 3(1)	0.595 0(2)
S(3)	0.344 9(2)	0.103 7(1)	0.427 6(2)
S(4)	0.206 0(2)	0.228 9(1)	0.607 6(2)
S(5)	0.603 5(2)	0.470 82(9)	−0.162 3(2)
S(6)	0.511 0(2)	0.629 27(8)	−0.010 5(2)
S(7)	0.721 9(2)	0.560 0(1)	−0.301 6(2)
S(8)	0.624 0(2)	0.717 3(1)	−0.156 5(2)
N(1)	0.926 5(4)	0.241 4(3)	0.088 7(5)
C(1)	0.212 0(6)	0.088 1(4)	0.471 8(6)
C(2)	0.157 1(6)	0.139 5(4)	0.546 9(6)
C(3)	0.476 9(7)	0.100 9(5)	0.602 8(8)
C(4)	0.478 0(7)	0.175 5(4)	0.684 2(7)
C(5)	0.371 9(8)	0.200 0(4)	0.741 7(7)
C(6)	0.570 7(8)	0.217 2(5)	0.705 0(7)
C(7)	0.633 8(6)	0.561 6(3)	−0.187 8(6)
C(8)	0.595 3(6)	0.626 5(3)	−0.127 1(6)
C(9)	0.601 7(9)	0.613 8(5)	−0.455 2(8)
C(10)	0.516 2(9)	0.734 5(4)	−0.339 4(8)
C(11)	0.487 5(7)	0.665 2(4)	−0.431 3(7)
C(12)	0.368 1(8)	0.651 3(5)	−0.492 3(8)
C(13)	0.898 6(6)	0.292 2(4)	−0.037 6(6)
C(14)	1.008 8(7)	0.330 3(4)	−0.034 4(7)
C(15)	0.970 4(8)	0.372 1(5)	−0.173(1)
C(16)	1.070(1)	0.415 1(6)	−0.177(1)
C(17)	1.042 3(6)	0.175 2(3)	0.103 4(6)
C(18)	1.025 3(6)	0.121 5(4)	−0.024 0(7)
C(19)	1.145 7(7)	0.058 0(4)	0.003 5(7)
C(20)	1.268 8(8)	0.084 8(5)	0.019(1)
C(21)	0.800 3(6)	0.210 5(3)	0.060 5(6)
C(22)	0.799 5(6)	0.158 3(4)	0.171 3(6)
C(23)	0.668 2(7)	0.129 4(4)	0.116 3(7)
C(24)	0.656 3(7)	0.077 1(5)	0.220 8(9)
C(25)	0.966 8(6)	0.287 5(4)	0.226 7(6)
C(26)	0.865 7(6)	0.357 3(4)	0.234 8(7)
C(27)	0.914 1(7)	0.397 2(4)	0.376 2(8)
C(28)	0.815 6(8)	0.467 6(5)	0.390 2(9)

Preparations.—*4-Methylene-2,6,8,10-tetrathiabicyclo*[5.3.0]-*dec-1(7)-ene-9-thione* **I**. Compound $[NEt_4]_2[Zn(dmit)_2]$ **1** (5.00 g, 6.9 mmol) was dissolved in dry tetrahydrofuran (thf) (200 cm^3), and 3-chloro-2-(chloromethyl)prop-1-ene (2.00 g, 16 mmol) added in one portion, under argon. The mixture was refluxed for 4 h, the flask sealed and the solution stirred at room temperature for 16 h. The orange solution was poured into deionised water (500 cm^3) to yield a dark coloured precipitate. The solution was stirred for 15 min and then stored at −10 °C for 2 h to ensure complete precipitation. The solid was filtered off, washed with water, acetone and air-dried to yield an olive green fibrous solid which was recrystallised from CH_2Cl_2–MeOH to afford the product as pale brown needles (2.66 g, 75%), m.p. 142–143 °C (Found: C, 33.90; H, 2.55; N, 0.00. $C_7H_6S_5$ requires C, 33.60; H, 2.40; N, 0.00%); *m/z* (EI) 250 (M^+, 100%); ^1H NMR ($CDCl_3$, $SiMe_4$) δ 5.3 (s, CH_2), 3.4 (s, CH_2); IR (KBr) 1064 cm^{-1} ν(C=S); UV/VIS (CH_2Cl_2) λ_{max}(ln ε) 369 (9.40), 270 (8.92), 230 nm (8.92).

4-Methylene-2,6,8,10-tetrathiabicyclo[5.3.0]*dec-1(7)-en-9-one* **II**. Compound **I** (2.00 g, 8 mmol) was dissolved in CH_2Cl_2 (150 cm^3) (HPLC grade), and glacial acetic acid (30 cm^3) added. Mercury(II) acetate (5.34 g, 16 mmol) was added and an almost instantaneous precipitation of HgS occurred, followed by a lightening in the colour of the solution. The flask was sealed and the mixture stirred at room temperature for 16 h. The precipitate was filtered off and washed with CH_2Cl_2. The orange organic phase was washed sequentially with saturated $NaHCO_3$ solution (3 × 150 cm^3) and deionised water (2 × 150 cm^3). The CH_2Cl_2 phase was dried over anhydrous Na_2SO_4, and then concentrated under vacuum to yield a solid orange residue. Recrystallisation from CH_2Cl_2–MeOH afforded the pure product as pale orange needles (1.58 g, 84%), m.p. 148–150 °C (Found: C, 35.95; H, 2.60; N, 0.00. $C_7H_6OS_4$ requires C, 35.90; H, 2.55; N, 0.00%); *m/z* (EI) 234 (M^+, 95%); ^1H NMR ($CDCl_3$, $SiMe_4$) δ 5.2 (s, CH_2), 3.3 (s, CH_2); IR (KBr) 1655 cm^{-1} ν(C=O); UV/VIS (CH_2Cl_2) λ_{max}(ln ε) 277 (8.90), 227 nm (8.43).

$[NBu_4][Ni(dpdt)_2]$ **2**. Compound **II** (1.00 g, 4 mmol) was suspended in EtOH (10 cm^3) under a dry argon atmosphere. Hexane washed sodium (0.19 g, 8.2 mmol) dissolved in EtOH (5 cm^3) was added to the suspension which was stirred at room temperature for 1 h. Then NBu_4Br (2.75 g, 8.5 mmol) dissolved in EtOH (10 cm^3) was added to the clear yellow solution, followed by dropwise addition of a solution of $NiCl_2 \cdot 6H_2O$ (0.50 g, 2.1 mmol) in EtOH (20 cm^3) over a 30 min period. After the addition was complete the dark brown solution was stirred for 1.5 h, reduced in volume under vacuum, and stored at −10 °C for 2 h. The dark brown precipitate was filtered off, washed with EtOH and air-dried. Recrystallisation from CH_2Cl_2–Pr^iOH afforded the product as a brown crystalline solid (1.22 g, 80%).

$[NBu_4][Au(dpdt)_2]$ **3**. Compound **II** (0.5 g, 2 mmol) was suspended in EtOH (10 cm^3) under a dry argon atmosphere. Hexane washed sodium (0.10 g, 4 mmol) dissolved in EtOH (5 cm^3) was added and the mixture stirred for 1 h. Then NBu_4Br (1.37 g, 4 mmol) dissolved in EtOH (5 cm^3) was added to the

yellow solution, followed by dropwise addition of a solution of $K[AuCl_4]\cdot 3H_2O$ (0.46 g, 1 mmol) in EtOH (20 cm^3). The solution darkened and gradually a pale brown solid precipitated. The mixture was stirred at room temperature for 1.5 h and the solid was filtered off, washed with EtOH and air-dried. Recrystallisation from acetone–Pr^iOH (1:1) yielded a golden brown crystalline solid (0.56 g, 62%).

$[NBu_4][Cu(dpdt)_2]$ **4**. Compound **II** (0.50 g, 2 mmol) was added to a mixture of EtOH (15 cm^3), and hexane washed sodium (0.10 g, 4 mmol), which was stirred at room temperature for 1 h. Then $CuCl_2\cdot 2H_2O$ (0.16 g, 1 mmol) dissolved in EtOH (3 cm^3) was added to the solution, which resulted in a colour change to red-brown, and the simultaneous precipitation of a dark brown solid. The solution was stirred for 1 h and NBu_4Br (1.37 g, 4.2 mmol) dissolved in EtOH (30 cm^3) added dropwise to the mixture. After the addition was complete the solution was stirred for 1.5 h, and the precipitate was filtered off, washed with EtOH and air-dried, to yield a dark red solid. Recrystallisation from acetone–diethyl ether (4:1) afforded the pure compound as a dark red crystalline solid (0.41 g, 54%).

$[NMe_4][Ni(dpdt)_2]$ **5**. This compound was prepared using the method described for the $[NBu_4][Ni(dpdt)_2]$ complex **2**, but starting from compound **II** (0.5 g). A brown crystalline solid was obtained (0.23 g, 40%).

$[Ni(dpdt)_2]$ **6**. Complex **2** (0.50 g, 0.7 mmol) was dissolved in acetone (50 cm^3) and iodine (0.06 g, 0.4 mmol) was added with stirring at room temperature. The solution was stirred for 30 min and then stored at −10 °C for 2 h. The light green powder was filtered off, washed with diethyl ether and air dried (0.17 g, 30%) (Found: C, 31.30; H, 2.60; N, 0.00. $C_{12}H_{12}NiS_8$ requires C, 30.60; H, 2.55; N, 0.00%).

Crystal-structure Determinations.—All measurements were made at room temperature on a Rigaku AFCSR diffractometer with graphite-monochromated Mo-Kα radiation and a 12 kW rotating anode generator at the Department of Chemistry, University of Tokyo, Japan.

Crystal data for $[NBu_4][Ni(dpdt)_2]$ **2**. $C_{28}H_{48}NNiS_8$, $M = 713.94$, triclinic, space group $P\bar{1}$, $a = 10.292(2)$, $b = 18.882(4)$, $c = 10.235(2)$ Å, $\alpha = 104.36(2)$, $\beta = 111.30(2)$, $\gamma = 81.97(2)°$, $U = 1792.4(8)$ Å^3, $Z = 2$, $D_c = 1.478$ g cm^{-3}, $F(000) = 744$. Black block. Crystal dimensions: 0.4 × 0.2 × 0.6 mm, μ(Mo-Kα) = 10.05 cm^{-1}.

Data collection and processing. Cell constants obtained from a least-squares refinement using 25 centred reflections in the range $32.36 < 2\theta < 36.82°$. Data were collected at 21 ± 1 °C, ω–2θ mode to a maximum 2θ value of 55.10°, with ω scan width = 1.10 + 0.30 tan θ, ω scan speed 6.0° min^{-1}. 8732 Reflections measured, 8721 were unique ($R_{int} = 0.039$). The data were corrected for Lorentz and polarisation effects.

Structure analysis and refinement. The structure was solved by direct methods,[28] with the non-hydrogen atoms being refined anisotropically. Full-matrix least-squares refinement was based on 2796 observed reflections [$I > 3.0\sigma(I)$] and 346 variable parameters and converged with R and R' values of 0.051 and 0.048. An empirical absorption correction, based on azimuthal scans of three reflections was applied which resulted in transmission factors ranging from 0.76 to 1.00. Neutral-atom scattering factors were taken from Cromer and Waber.[29] Anomalous dispersion effects were included in F_c. All calculations were performed using the TEXSAN[30] crystallographic package.

Crystal data for $[NBu_4][Au(dpdt)_2]$ **3**. $C_{28}H_{48}AuNS_8$, $M = 852.23$, triclinic, space group $P\bar{1}$, $a = 11.058(2)$, $b = 17.569(3)$, $c = 10.144(2)$ Å, $\alpha = 94.56(2)$, $\beta = 112.23(1)$, $\gamma = 78.74(2)°$, $U = 1789.1$ Å^3, $Z = 2$, $D_c = 1.583$ g cm^{-3}, $F(000) = 846$. Yellow block. Crystal dimensions: 0.3 × 0.4 × 0.5 mm, μ(Mo-Kα) = 45.61 cm^{-1}.

Data collection and processing. Data collected using ω–2θ mode with ω scan width = 1.47 + 0.30 tan θ, ω scan speed 24.0° min^{-1}. 10 999 Reflections collected, 10 497 were unique ($R_{int} = 0.026$) [absorption correction resulted in max., min. transmission factors = 1.00, 0.63].

Structure solution and refinement. Structure was solved by direct methods, and non-hydrogen atoms refined anisotropically. Full-matrix least-squares refinement was performed using 5359 independent reflections [$I > 3.0\sigma(I)$] and 346 parameters. The R and R' values were 0.034 and 0.035 respectively. Programs used and sources of scattering factor data are detailed elsewhere.[28–30]

Crystal data for $[NBu_4][Cu(dpdt)_2]$ **4**. $C_{28}H_{48}CuNS_8$, $M = 718.72$, triclinic, space group $P\bar{1}$, $a = 10.263(4)$, $b = 18.938(5)$, $c = 10.253(6)$ Å, $\alpha = 98.35(3)$, $\beta = 111.17(3)$, $\gamma = 75.09(2)°$, $U = 1793(1)$ Å^3, $Z = 2$, $D_c = 1.331$ g cm^{-3}, $F(000) = 760$. Black block. Crystal dimensions = 0.5 × 0.37 × 0.37 mm, μ(Mo-Kα) = 10.77 cm^{-1}.

Data collection and processing. Data were collected at 23 ± 1 °C, ω–2θ mode with ω scan width = 1.15 + 0.30 tan θ, ω scan speed 8.0° min^{-1}. 8753 Reflections collected, 8291 were unique ($R_{int} = 0.024$) [absorption correction resulted in max., min. transmission factors = 1.00, 0.95].

Structure solution and refinement. Structure was solved by a combination of Patterson and direct methods. Full-matrix least-squares refinement was based on 3484 independent reflections [$I > 3.0\sigma(I)$] and 346 variable parameters. The R and R' values were 0.045 and 0.047 respectively. The weighting scheme was $w = 1/\sigma(F)^2$ in each case. Programs used and sources of scattering factor data are detailed elsewhere.[28–30]

Additional material available from the Cambridge Crystallographic Data Centre comprises thermal parameters.

Acknowledgements

We thank Dr. J. Møller (Odense University, Denmark) for running the FAB mass spectra, Dr. R. H. Friend and Mr. T. Coomber (University of Cambridge) for magnetic measurements and the SERC for provision of a Studentship (to A. C.) and the British Council for support.

References

1 A. E. Underhill, *J. Mater. Chem.*, 1992, **2**, 1; M. R. Bryce, *Chem. Soc. Rev.*, 1991, **20**, 355; R.-M. Olk, B. Olk, W. Dietzsch, R. Kirmse and E. Hoyer, *Coord. Chem. Rev.*, 1992, **117**, 99.
2 P. Cassoux, L. Valade, H. Kobayashi, A. Kobayashi, R. A. Clark and A. E. Underhill, *Coord. Chem. Rev.*, 1992, **110**, 115.
3 L. Brossard, M. Ribault, L. Valade and P. Cassoux, *J. Phys. (Paris)*, 1989, **50**, 1521; A. Kobayashi, H. Kim, Y. Sasaki, R. Kato, H. Kobayashi, S. Moriyama, Y. Nishio, K. Kajita and W. Sasaki, *Chem. Lett.*, 1987, 1819; A. Kobayashi, R. Kato, A. Miyamoto, T. Naito, H. Kobayashi, R. A. Clark and A. E. Underhill, *Chem. Lett.*, 1991, 2163; H. Kobayashi, K. Bun, T. Naito, R. Kato and A. Kobayashi, *Chem. Lett.*, 1992, 1909.
4 P. Cassoux and L. Valade, in *Inorganic Materials*, eds. D. W. Bruce and D. O'Hare, Wiley, Chichester, 1992.
5 L. Brossard, M. Ribault, L. Valade and P. Cassoux, *Physica B & C (Amsterdam)*, 1986, **143**, 378.
6 H. Tajima, M. Inokuchi, A. Kobayashi, T. Ohta, R. Kato, H. Kobayashi and H. Kuroda, *Chem. Lett.*, 1993, 1235.
7 For example, I. Hawkins and A. E. Underhill, *J. Chem. Soc., Chem. Commun.*, 1990, 1594; O. A. Dyachenko, V. V. Gritsenko, G. V. Shilov, E. E. Laukina and E. B. Yagubskii, *Synth. Met.*, 1993, **58**, 137; H. Kim, A. Kobayashi, Y. Sasaki, R. Kato, H. Kobayashi, T. Nakamura, T. Nogami and Y. Shirota, *Bull. Chem. Soc. Jpn.*, 1988, **61**, 2559.
8 G. Steimecke, H.-J. Sieler, R. Kirmse and E. Hoyer, *Phosphorus Sulfur Relat. Elem.*, 1979, **7**, 49.
9 J. D. Forrester, A. Zalkin and D. H. Templeton, *Inorg. Chem.*, 1964, **3**, 1507.
10 C. T. Vance, J. H. Welch and R. D. Bereman, *Inorg. Chim. Acta*, 1989, **164**, 191.
11 G. Matsubayashi, K. Takahashi and T. Tanaka, *J. Chem. Soc., Dalton Trans.*, 1988, 967.
12 R. Kato, H. Kobayashi, A. Kobayashi and Y. Sasaki, *Bull. Chem. Soc. Jpn.*, 1986, **59**, 627.

13 A. Charlton, A. E. Underhill, K. M. A. Malik, M. B. Hursthouse, T. Jørgensen and J. Becher, *Synth. Met.*, 1995, **68**, 221.
14 (*a*) A. J. Schultz, H. H. Wang, L. C. Soderholm, T. L. Sifter, J. M. Williams, K. Bechgaard and M.-H. Whangbo, *Inorg. Chem.*, 1987, **26**, 3757; (*b*) J. H. Welch, R. D. Bereman and P. Singh, *Inorg. Chem.*, 1988, **27**, 3680.
15 O. Lindquist, L. Andersen, J. Sieler, G. Steimecke and E. Hoyer, *Acta Chem. Scand., Ser. A*, 36, 1982, **10**, 855.
16 G. N. Schrauzer, *Acc. Chem. Res.*, 1969, **2**, 72.
17 L. Valade, J.-P. Legros, M. Bousseau, P. Cassoux, M. Garbauskas and L. V. Interrante, *J. Chem. Soc., Dalton Trans.*, 1985, 783.
18 G. Matsubayashi and A. Yokozawa, *J. Chem. Soc., Dalton Trans.*, 1990, 3535.
19 U. T. Mueller-Westerhoff and B. Vance, *Comprehensive Co-ordination Chemistry*, eds. G. Wilkinson, R. D. Gillard and J. A. McCleverty, Pergamon, Oxford, 1987, vol. 6, p. 595; J. Fabian, H. Nakazumi and M. Matusoka, *Chem. Rev.*, 1992, **92**, 1197.
20 (*a*) D. C. Olson, V. P. Mayweg and G. N. Schrauzer, *J. Am. Chem. Soc.*, 1966, **88**, 4876; (*b*) M. J. Baker-Hawkes, E. Billig and H. B. Gray, *J. Am. Chem. Soc.*, 1966, **88**, 4870; (*c*) G. A. Bowmaker, P. D. W. Boyd and G. K. Campbell, *Inorg. Chem.*, 1983, **22**, 1208.
21 M. Bousseau, Ph.D. Thesis, Toulouse University, 1984.
22 E. B. Yagubskii, A. I. Kotov, E. E. Laukhina, A. A. Ignatiev, I. I. Buravov and A. G. Khomenko, *Synth. Met.*, 1991, **41–43**, 2515.
23 N. C. Schiødt, T. Bjørnholm, C. S. Jacobsen and K. Bechgaard, *Synth. Met.*, 1993, **56**, 2164.
24 T. Nakamura, T. Nogami and Y. Shirota, *Bull. Chem. Soc. Jpn.*, 1987, **60**, 3447.
25 R. A. Clark, Ph.D. Thesis, University of Wales, Bangor, 1990.
26 C. T. Vance and R. D. Bereman, *Inorg. Chim. Acta*, 1988, **149**, 229.
27 M. Adam, U. Scherer, Y.-J. Shen and K. Müllen, *Synth. Met.*, 1993, **56**, 2108.
28 J. C. Calbrese, PHASE, 'Patterson Heavy Atom Solution Extractor', Ph.D. Thesis, University of Wisconsin, Madison, 1972; P. T. Beurskens, DIRDIF, Direct Methods for PHASE Extension and Refinement of Difference Structure Factors, Technical Report, Crystallography Laboratory, Toernooiveld, Nijmegen, 1984.
29 D. T. Cromer and J. T. Waber, *International Tables for X-Ray Crystallography*, Kynoch Press, Birmingham, 1974, vol. 4, Table 2.2A.
30 TEXSAN-TEXRAY Structural Analysis Package, Molecular Structure Corporation, Houston, TX, 1985.

Received 13*th September* 1994; *Paper* 4/05558F